METAL-OXIDE-METAL POINT CONTACT JUNCTION DETECTORS

Final Technical Report

N.A.S.A. Contract # NGR 06-003-160

Period Covered: 1 September 1970-31 August 1973

Prepared by: Dr. Jack Baird, Project Director
R. H. Havemann, Research Assistant
R. D. Fults, Research Assistant

Department of Electrical Engineering
University of Colorado
Boulder, Colorado 80302

ABSTRACT

This is the final report on a study of metal-oxide-metal point contact junction detectors. The objectives were to resolve the detection mechanism(s) and to design a mechanically stable detector. During the contract period the following work has been accomplished:

(1) Detection can be attributed to two mechanisms which occur simultaneously;

(2) A prototype for a mechanically stable device has been constructed and tested;

(3) A technique has been developed which accurately predicts microwave video detector and heterodyne mixer SIM (semiconductor-insulator-metal) diode performance from low frequency I-V curves.

Research in the above areas is continuing. Detailed results will be published as technical papers and submitted as appendices to this paper.

METAL-OXIDE-METAL POINT CONTACT JUNCTION DETECTORS

The objectives of this study of metal-oxide-metal (MOM), also known as metal-insulator-metal (MIM), point contact junction detectors were to resolve the detection mechanism(s) and to design a mechanically stable detector. During the contract period the following work has been accomplished:

(1) Detection can be attributed to two mechanisms which occur simultaneously;

(2) A prototype for a mechanically stable device has been constructed and tested;

(3) A technique has been developed which accurately predicts microwave video detector and heterodyne mixer SIM (semiconductor-insulator-metal) diode performance from low frequency I-V curves.

As of this date, all work is still in progress. Detailed final results will be contained in R. Havemann's Dissertation and R. Fults' Masters Thesis, both to be published in May 1974. However, at least two papers, one on the MOM detection theory and another on the SIM microwave diode performance prediction technique, should be finished by the end of this year. Since detailed results will be published as technical papers, this report will summarize the directions this research has taken and the conclusions that have evolved.

For many years, the dominant detection mechanism for MOM detectors has been attributed to a difference in contact

potential first analyzed correctly by Simmons[1-5]. Based on the tunneling theory of Stratton[6] and Simmons, Coleman and Green[7] developed a theory which explained zero bias detection in a MOM junction. If the two metals on either side of the tunneling barrier have different contact potentials, an effective bias (but no DC current or associated shot noise) is produced which introduces an asymmetry in the current-voltage relationship. According to Coleman and Green, this asymmetry suffices to explain the observed responsivity (volts output per watt input) regardless of frequency, at least until the reactance of the junction becomes important. Thus, if it were possible to trace a typical MOM I-V curve at, say, microwave frequencies, the curve should be identical with the low frequency (DC) characteristic. However, even allowing for the effective bias of the MOM detector, the observed low frequency MOM I-V curves are far less nonlinear than their SIM counterparts of comparable responsivity as shown in Figure 1.

Based upon this apparent anomaly, the following explanations could be proposed:

(1) High frequency detector behavior cannot be predicted from low frequency I-V curves;

(2) A detection mechanism is present which is either frequency dependent and/or does not appear in I-V curves at any frequency.

The first goal of this research was to verify that the high frequency (microwave) performance of a SIM detector could be predicted from the low frequency (~DC) I-V curves.

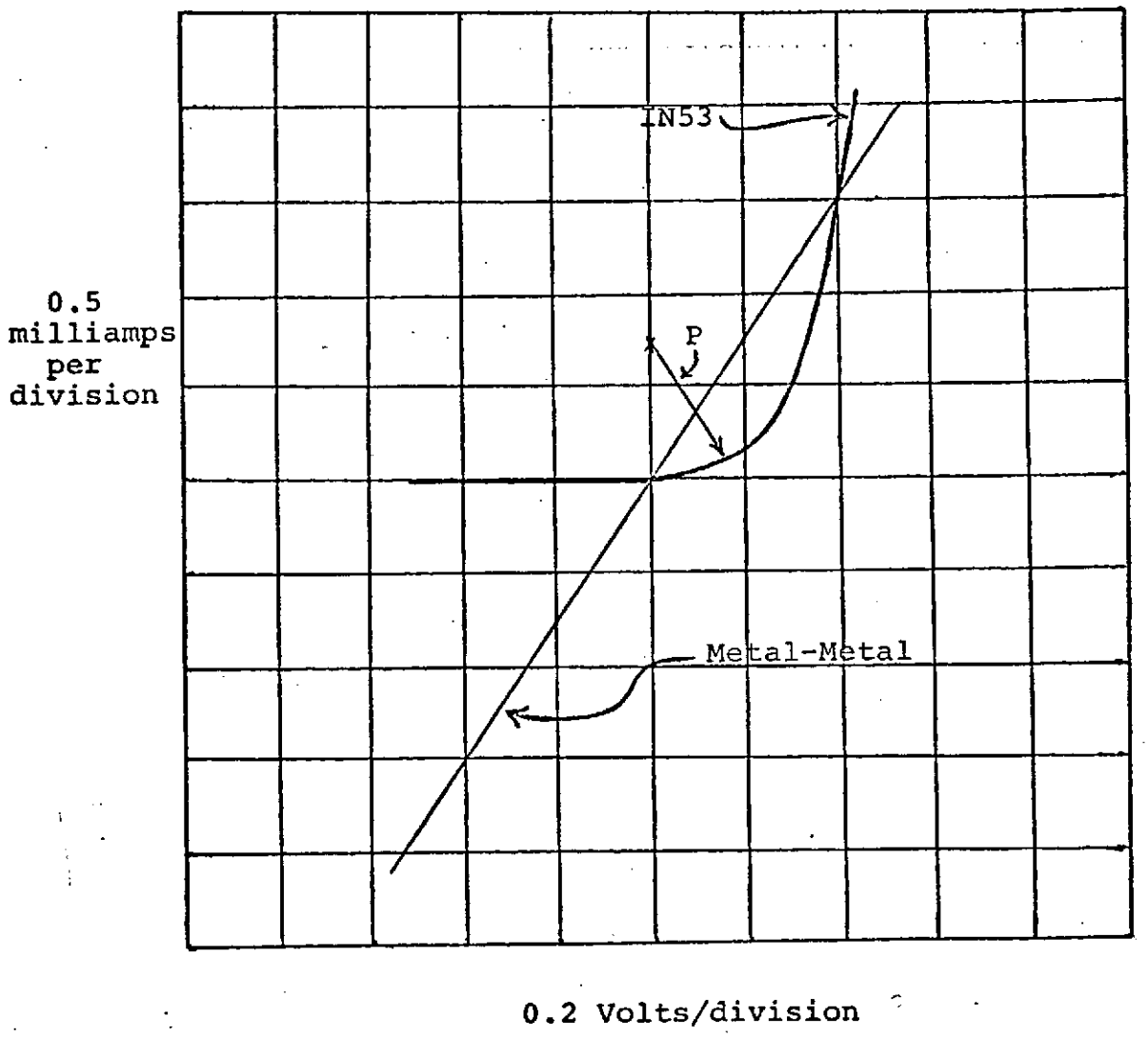

Figure 1. Comparison of SIM and MOM I-V Characteristics

If this could be shown, then it would be implausible to expect a frequency independent effect such as a difference in contact potential to be the sole detection mechanism, since the responsivities inferred from the curves of Figure 1 could not possibly be the same, even allowing for the "effective bias" of the MOM junction. With this objective in mind, a technique was developed which accurately predicts the performance of a SIM microwave video detector and heterodyne mixer strictly from the DC characteristics of the diode.

In order to explain the theory behind this technique, consider the following Maclaurin series expansion of the current i as a function of voltage v:

$$i(v) = Av + Bv^2 + Cv^3 + Dv^4 + Ev^5 + Fv^6 + \ldots \quad . \qquad (1)$$

Earlier authors[7] have shown that the responsivity of a square-law video detector can be determined from the first two coefficients in the above expansion. Note that A and B may be determined directly from the diode I-V curve since A corresponds to the slope at the origin and B is proportional to the second derivative at the origin. However, higher order terms are necessary to correctly describe behavior for departures from square-law operation. Indeed, beyond the square-law region the first two coefficients indicate a behavior decidedly opposite experimental observation.

Consequently the circuit of Figure 2 was constructed using analog multiplier circuits to simulate an I-V curve according to Equation (1). By matching the true diode I-V characteristics

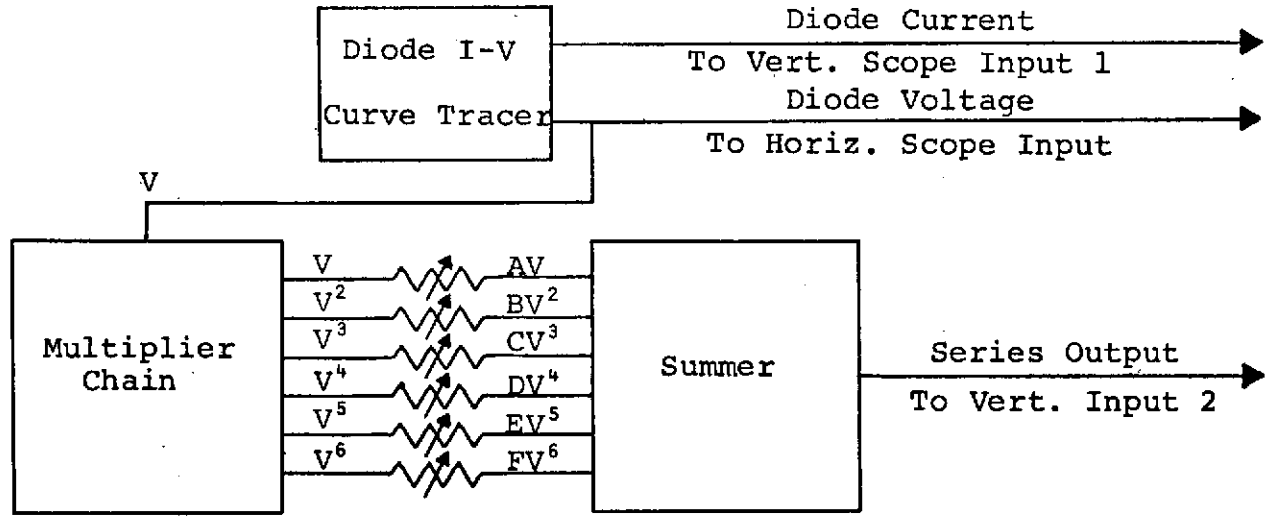

Figure 2. I-V Curve Tracer and Simulator

with the simulated I-V curve, the unique coefficients describing the diode can be determined. In practice, the first six coefficients appear to provide enough information to describe microwave video detector and mixer performance over power levels of normal use. Once the coefficients have been obtained, the relevant microwave parameters such as detectivity of the video detector or the conversion loss, tangential signal sensitivity, and IF impedance of the mixer can be calculated according to the theory outlined below.

Consider the equivalent circuit of a simple video detector shown in Figure 3(a). A DC voltage of V_0 is developed across the diode due to the application of an AC voltage $V\sin\omega t$; thus the voltage across the detector is necessarily given by

$$v = V_0 + V\sin\omega t \qquad (2)$$

The DC current through the diode is $-V_0/(R_L+Z_o)$. Substituting for v in Equation (1) and equating DC terms on both sides of the equation yields

$$DV_0^4+CV_0^3+(B+3DV^2)V_0^2+\left(A+\frac{1}{R_L+Z_o}+\frac{3}{2}CV^2\right)V_0+\frac{1}{2}BV^2+\frac{3}{8}DV^4 = 0 \quad . \qquad (3)$$

For small V and V_0, the output voltage of the video detector (including impedance mismatch effects) is given by

$$V_0 = \frac{-4BZ_oP^+}{A+\frac{1}{R_L+Z_o}}\left\{1 - \frac{12CZ_oP^+}{A+\frac{1}{R_L+Z_o}} - \ldots\right\} \qquad (4)$$

where P^+ is the incident microwave power. Note that for large R_L, the departure from square-law behavior occurs when the

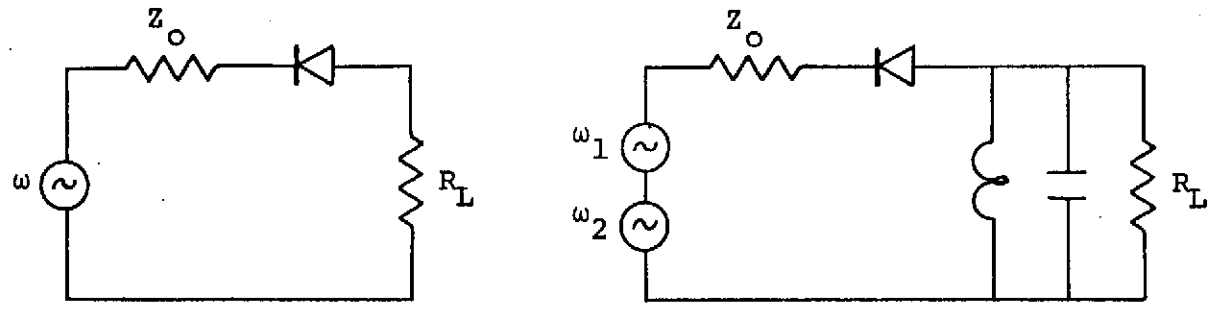

Figure 3. Equivalent Circuits for Video Detector and Heterodyne Mixer

incident power approaches the same order of magnitude as the term $A/12CZ_o$. Thus, the square-law response of a video detector can be predicted from the first two coefficients of Equation (1), but the third coefficient (C) is required to describe departure from square-law behavior. Values of detectivity predicted from Equation (4) using A and B coefficients measured by the circuit of Figure 2 have been experimentally verified within 5% for 1N21 and 1N23 diodes at microwave frequencies below the corner frequency attributed to diode reactance. The nature of the departure from the square-law region has also been verified.

Now consider the equivalent circuit of a simple heterodyne mixer shown in Figure 3(b). Since the tank circuit appears as a short to the local oscillator at ω_1 as well as the signal at ω_2, the voltage across the detector is

$$v = V_1\sin(\omega_1 t) + V_2\sin(\omega_2 t) + V_3\sin(\omega_3 t + \theta_3) \qquad (5)$$

Substituting (5) for v in Equation (1), equating terms in ω_3 and solving for V_3, assuming $v_1 >> V_2$, V_3 yields

$$V_3 = \frac{V_1 V_2 (B+\frac{3}{2}DV_1^2+\frac{15}{8}FV_1^4)}{\frac{1}{R_L}+A+\frac{3}{2}CV_1^2+\frac{15}{8}EV_1^4} \quad . \qquad (6)$$

Note that the DC current I_0, local oscillator current I_1 and signal current I_2 may be obtained in a similar manner by equating coefficients in $\omega=0$, ω_1, and ω_2, respectively. Converting Equation (6) from voltage to power readily yields an expression for P_2/P_3, a measure of the conversion loss. Since I_0 can be

determined, the shot noise and tangential signal sensitivity may be calculated.

Using the circuit of Figure 2 the coefficients in expansion (1) were experimentally determined for a typical 1N21C microwave diode. The tangential signal sensitivity and conversion gain as a function of local oscillator power, given by Figures 4 and 5, respectively, were predicted from the measured DC parameters. Thus, the performance of a microwave diode both as a video detector and heterodyne mixer can be predicted from the DC I-V characteristics. It should be noted that this prediction technique offers considerable advantage in time and simplicity over current methods of determining video detector and heterodyne mixer characteristics from measurements taken at microwave frequencies.

Once it had been verified that high frequency detector behavior could be accurately predicted from low frequency I-V curves, the next step was twofold -- first, the previous theory based on a difference in contact potential needed to be examined in detail and second, other theories needed to be considered which might possibly explain the observed anomalies. Examination of the contact potential difference theory is the topic of R. Fults' Masters Thesis and is currently still in progress. However, at present there is reason to believe that earlier studies have overlooked the dominant terms in applying Simmon's theory to the MOM detector. This question will be resolved in the thesis.

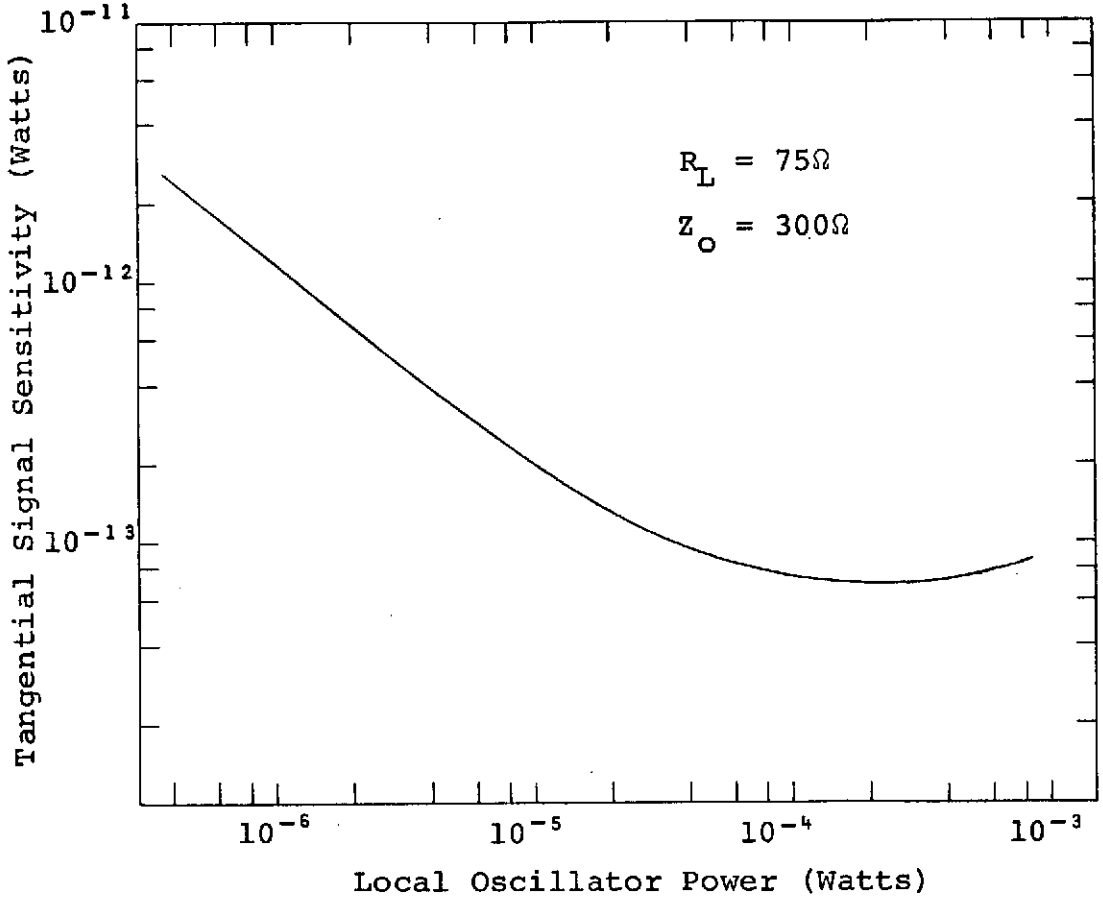

Figure 4. Tangential Signal Sensitivity vs. Local Oscillator Power

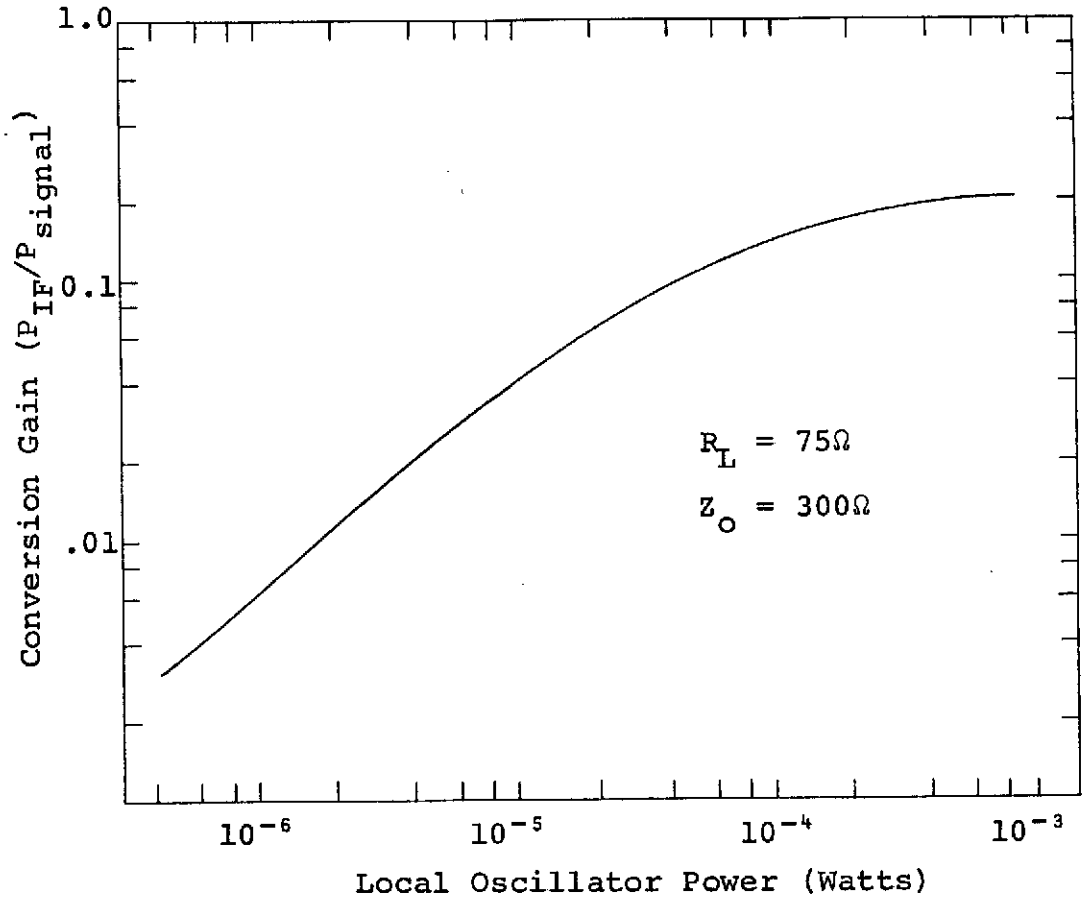

Figure 5. Conversion Gain vs. Local Oscillator Power

In order to explain the discrepancies between experimental observations and the contact potential difference theory, a thorough examination of alternative theories was undertaken. An alternate theory was found, and this is the subject of R. Havemann's Dissertation. This theory predicts the correct magnitude of short-circuit current for MOM devices, but the exact calculation of the open circuit voltage is not complete at this time. An approximate calculation of the open circuit voltage agrees with experimental observations. As has been mentioned, a detailed presentation of this theory will be submitted for publication by the end of this year. What follows is a general description of the theory and its consequences.

Specifically, it can be shown that when conductor geometry constrains internal AC fields to have significant spatial gradients over one mean free path, then the strictly linear relation between current density and electric field given by Ohm's law ($J=\sigma E$) is no longer valid. Rather, the current density should be calculated from the expanded distribution function that is dependent both on orders of the applied AC electric field and spatial gradients of the distribution function. At low frequencies ($\omega\tau<<1$) the Boltzmann transport equation for the electron distribution function $f(\vec{r},\vec{k},t)$ may be written

$$\vec{v}\cdot\nabla_r f + \vec{F}\cdot\nabla_k f = -\frac{f-f_o}{\tau} \quad , \tag{7}$$

where the relaxation approximation has been used and the equilibrium distribution function f_o is assumed to be independent of $\vec{r}$. The force $\vec{F}$ was assumed to be due to a position and time

dependent electric field $\vec{E}$, and the relaxation time τ was assumed to be constant.

An approximate solution to the Boltzmann equation was obtained by using a double perturbation technique in which the distribution function f was perturbed by the electric field amplitude and spatial gradients of f. To second order in $\vec{E}$ and to first order in spatial gradients of f, the solution of Boltzmann's equation yields the following result for current density:

$$J = \sigma\vec{E} - \frac{e\tau^2}{m}\sigma\{3\vec{E}(\nabla\cdot\vec{E}) + 2(\vec{E}\cdot\nabla)\vec{E}\} \qquad (8)$$

where

$$\sigma = \frac{1}{3\pi^2}\frac{e^2\tau}{m}k_F^3 = n|e|\mu \quad \text{and} \quad \vec{E} = \vec{E}_o(x,y,z)\sin\omega t.$$

The first term of equation (8) is the standard form of Ohm's law. In order to illustrate the physical significance of the second term, consider the AC electric field configuration shown in Figure 6. This geometry represents an idealized approximation to a typical MOM device. In many cases the whisker diameter will be of the order of one mean free path or less, and the radius of curvature of the electric field will be significant over a distance of one mean path. Under these circumstances, electrons cannot follow the electric field, that is, Ohm's law no longer yields the correct current density and, to a first approximation, equation (8) must be used to calculate $\vec{J}$. At greater power levels (stronger $\vec{E}$ fields), higher order approximations would be necessary, but equation (8) should be valid for power levels corresponding to square-law operation.

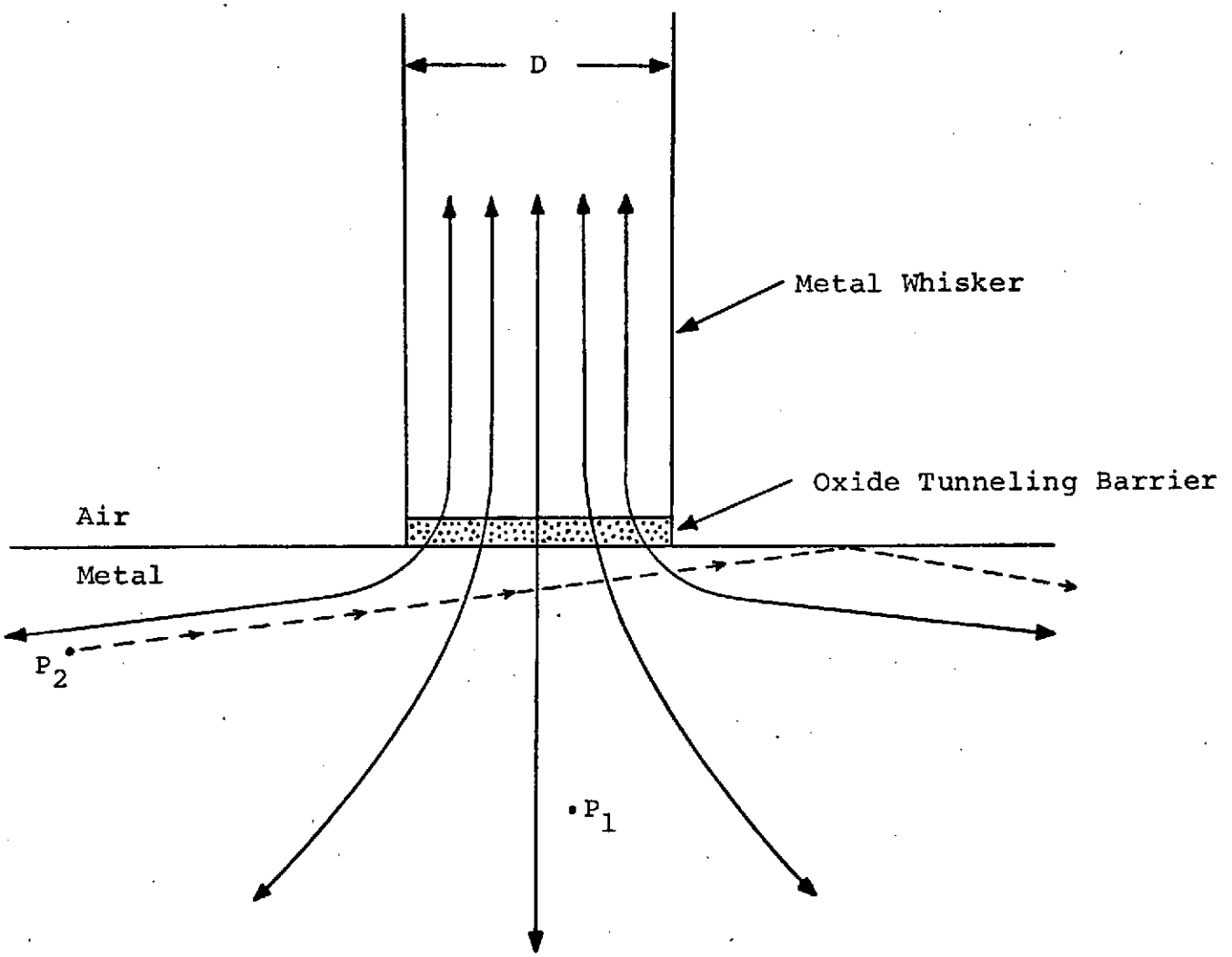

Figure 6. Idealized Detector Electric Field Configuration

Since electrons cannot follow a field whose radius of curvature is comparable to one electron mean free path, heuristically one would expect an asymmetry in the J vs. E relationship for the field configuration shown in Figure 6. Indeed, electrons do not need to follow the field in the substrate in order to tunnel out of the whisker into the substrate. Similarly, an electron at P_1 should be able to follow the field towards the whisker and be in a position to tunnel back into the whisker. However, the path of an electron at point P_2 will have to curve appreciably within one mean free path or the electron will miss the barrier completely and be reflected from the surface of the substrate. The dashed line in Figure 6 illustrates the path an electron at P_2 might follow if the AC electric field curvature is too stringent. Thus a DC current, or net flow of electrons out of the whisker, would be expected. For an AC electric field, this DC current is readily obtained from the second term of Equation (8). Note that in general, a DC current will be induced by either curvature of the AC field within one mean free path or by the divergence of an AC field. However, in each case a component of DC current will be perpendicular to the barrier.

In order to ascertain whether or not this geometric effect could contribute significantly to MOM detection, an order of magnitude calculation of the short-circuit current was performed. A 50Ω coaxial line supporting 1μ Watt of rf power was assumed to be terminated by a MOM detector operating into an open circuit. If the radius of curvature of electric

field is assumed comparable to a whisker diameter of 500 Å, then a current of approximately 1μ amp flows across the junction.

The open circuit voltage may be inferred from the short-circuit current by utilizing the linearized tunneling equations of Simmons in the limit of small voltage and current. The high (rf) frequency I-V curve at the external terminals can be viewed as a DC I-V curve which has been shifted according to Figure 7. In the vicinity of the origin over which this approximation is valid, the slope of the I-V curve is essentially constant (no curvature) and equal to $1/R_T$, where R_T is the tunneling resistance. However, since a geometrically-induced current has been shown to flow under short-circuit (V=0) conditions, then conversely a voltage must exist across the device under open-circuit (I=0) conditions. The open-circuit voltage can be determined from the short-circuit current and slope ($1/R_T$) in the vicinity of the origin. In a typical MOM detector, the tunneling resistance is of the order of 1K ohm. Using the value of short-circuit current calculated previously (1μ amp), an open-circuit voltage of 1m Volt is predicted. Thus, the equivalent detectivity of this device is 1000 Volts/-Watt. Although this model is a rather naïve one, it does serve to illustrate the significance and pertinence of geometrically-induced detection. The precise nature of the high frequency I-V curve must, of course, be determined by incorporating the geometric effect into Simmon's original tunneling theory. This calculation is presently near completion and will be published at a later date.

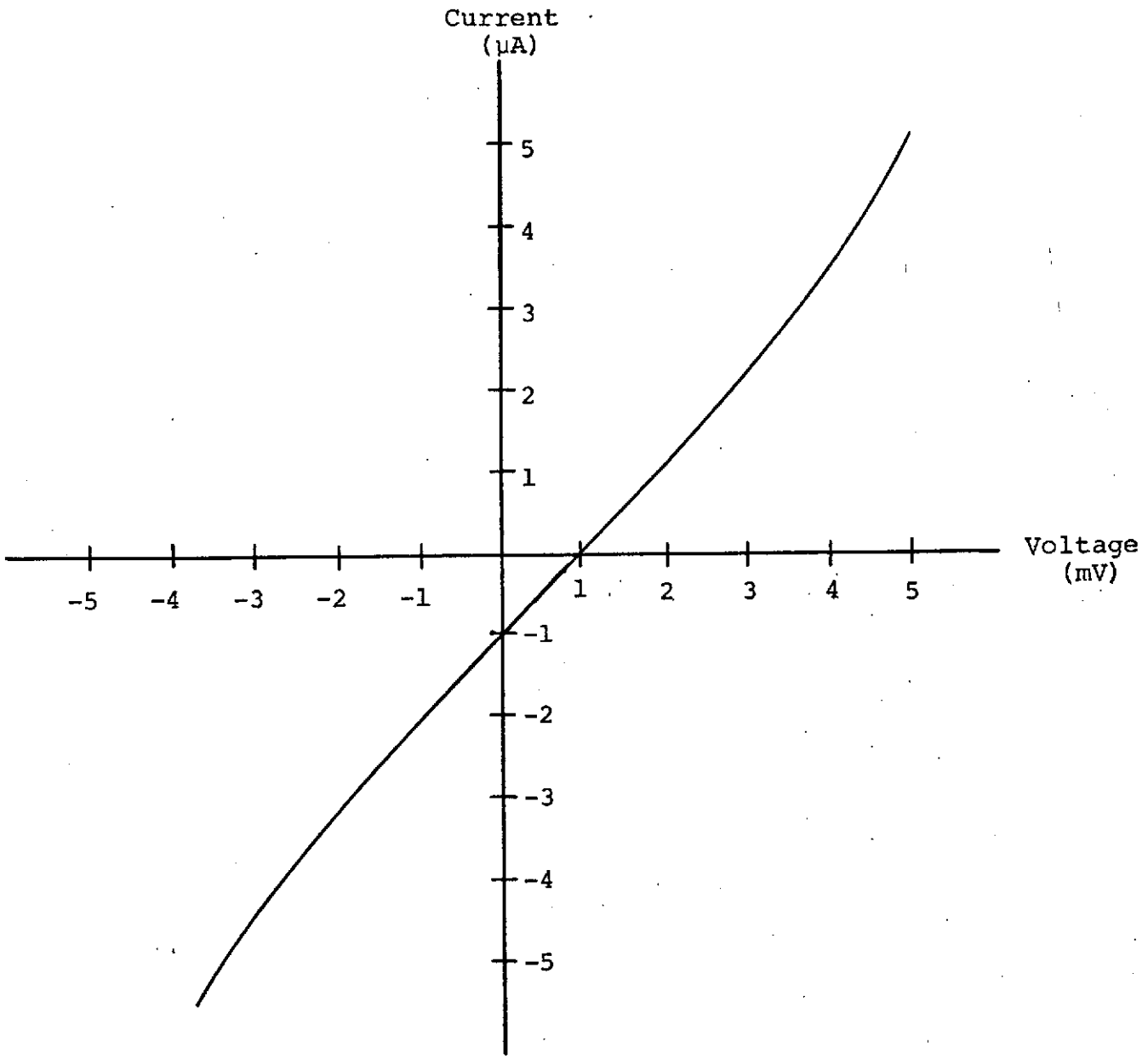

Figure 7. Hypothetical High (Microwave) Frequency I-V Curve

Several remarks should be made regarding the nature of geometrically-induced rectification. First, since the rectified current does not strictly follow the AC field, but obeys the vector relations shown in the second term of equation (8), one would not necessarily expect the geometric effect to appear in low or high frequency I-V traces. Actually, the situation is more complex than can be described by the short-circuit current "order of magnitude" calculation above since the tunneling barrier cannot be ignored. The I-V relation which includes geometric effects is currently being derived from Simmon's original tunneling theory. At this time, it appears that geometric effects can be related to an effective tunneling resistance, but the calculations are not yet complete.

Secondly, it should be noted that geometrically-induced rectification or detection can be enhanced by at least three methods:

(1) Increasing the frequency of operation until skin effect constraints force greater field curvature;

(2) Designing conductor geometry such that AC electric fields are constrained to have significant spatial gradients over one mean free path;

(3) Increasing the mean free path of an electron in the metal, thereby increasing the "effective electric field curvature".

Note that in each case the emphasis is upon increasing the effective electric field curvature over distances of one electron mean free path. Conductor geometries having sharp corners are therefore highly desirable. At microwave frequencies, the skin depth effect has only a small influence on field curvature over a distance of one mean free path, but skin effects could be significant at higher (infrared) frequencies. One obvious way of forcing electric field curvature to be significant over one mean free path is to use a thin film substrate with thickness on the order of a mean free path. Power dissipation might be a problem here, but non-conducting heat sinks (synthetic diamond, for example) are available and have been used in other devices. Of course optimum detection at any frequency or geometry will occur at cryogenic temperatures, since the electron mean free path will be longer and the "effective electric field curvature" will therefore be greater. It is felt that once the analysis is complete and the detection mechanism is understood, mechanically stable detectors can be designed for optimum detection by utilizing the above techniques to enhance geometrically-induced rectification.

Although much of this work is still in the theoretical state, considerable experimental effort has been concurrently devoted to the problem of fabricating a mechanically stable MOM detector. One configuration, illustrated in Figure 8, has produced some very encouraging results.

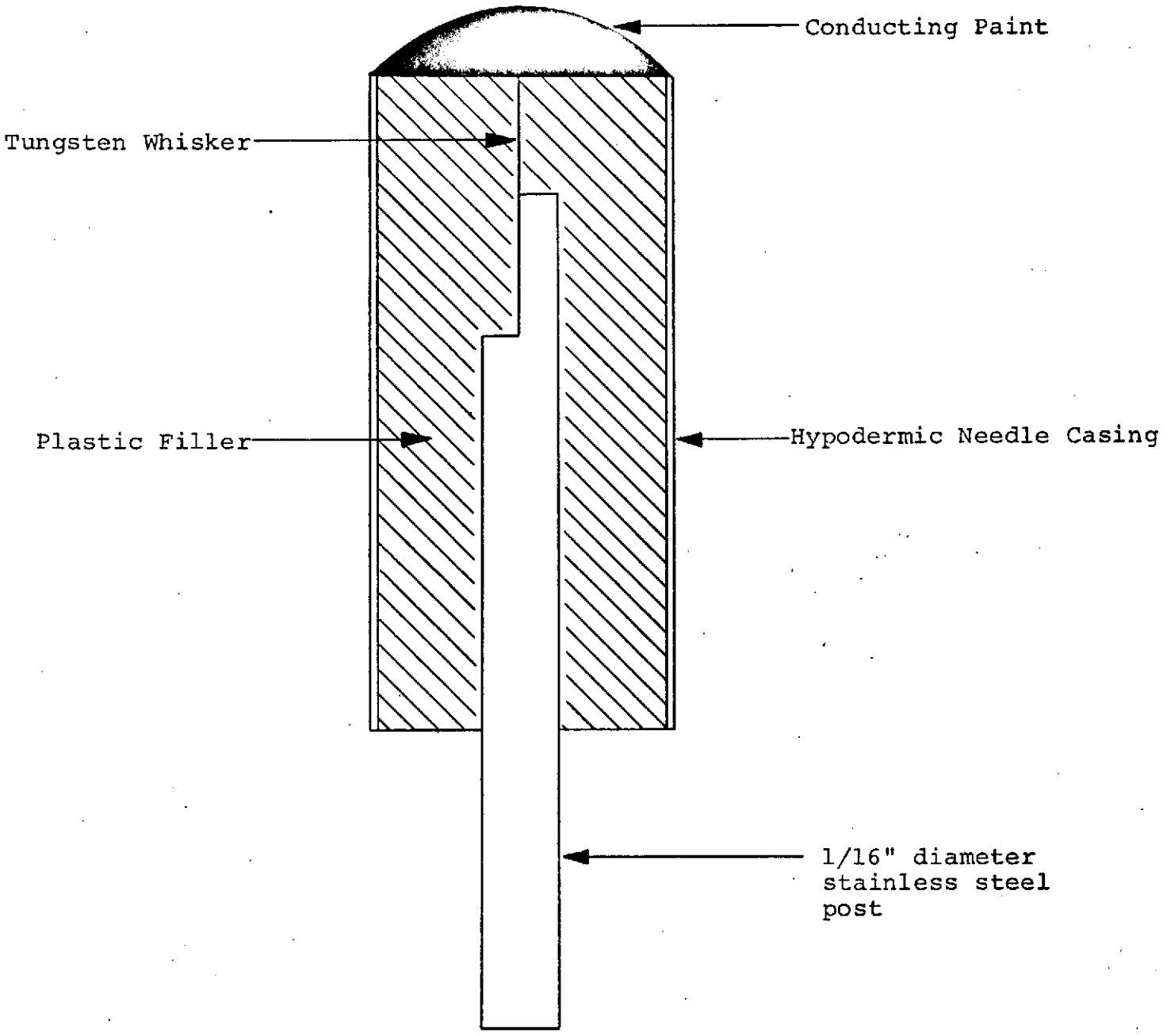

Figure 8. Prototype for Mechanically Stable MOM Detector

A small diameter (less than 0.001 inch) tungsten wire is welded to a 1/16 inch diameter stainless steel post and the wire is electrolytically pointed. The whisker and post are then inserted inside a section of hypodermic tubing and a liquid plastic material is injected so as to completely enclose the whisker tip. After the plastic has hardened, the right-hand end of the unit is polished until just the tip of the whisker is exposed. The entire end is then covered with a small drop of silver conducting paint. When RF energy is applied to the resulting coaxial structure, detection does occur. The mechanical stability is excellent but the detectivity is low since the dominant detection mechanism for this geometry is the difference in contact potential between the two metals. Several thin film designs which utilize geometrically-induced rectification as the dominant detection mechanism are presently being considered as possible prototypes for future devices. Refinements of these designs are awaiting the completion of the theoretical analysis of geometrically-induced rectification as applied to a tunneling junction.

In summary, the detection of electromagnetic radiation by a metal-oxide-metal tunneling junction can be attributed to two mechanisms -- a difference in contact potential between the two metals and a geometrically-induced rectification. Adaptation of the theory of geometrically-induced rectification to a tunneling junction is still in progress, but a paper will be written containing a detailed analysis of this effect upon completion of the necessary calculations. Once theoretical studies

are finished, work will continue on the problem of designing a mechanically stable MOM detector with high responsivity. In addition, a paper on the technique of predicting video detector and heterodyne mixer SIM diode performance from DC characteristics is also in progress. These papers will be subsequently submitted as appendices to this report. The final detailed summary of this research will be contained in R. Fults' Masters Thesis and R. Havemann's Dissertation.

REFERENCES

1. J. G. Simmons, "Generalized Formula for the Electric Tunnel Effect Between Similar Electrodes Separated by a Thin Insulating Film," Journal of Applied Physics, Vol. 34, pp. 1793-1803, June 1963.

2. J. G. Simmons, "Electric Tunnel Effect Between Dissimilar Electrodes Separated by a Thin Insulating Film," Journal of Applied Physics, Vol. 34, pp. 2581-2590, September 1963.

3. J. G. Simmons, "Potential Barriers and Emission Limited Current Flow Between Closely Spaced Parallel Metal Electrodes," Journal of Applied Physics, Vol. 35, pp. 2472-2481, August 1964.

4. J. G. Simmons, "Generalized Thermal J-V Characteristics for the Electric Tunnel Effect," Journal of Applied Physics, Vol. 35, pp. 2655-2658, September 1964.

5. J. G. Simmons, "The Electric Tunnel Effect and its Use in Determining Properties of Surface Oxides," Transactions of the Metallurgical Society of the AIME, Vol. 233, pp. 485-497, March 1965.

6. R. Stratton, "Volt-Current Characteristics for Tunneling Through Insulating Films," Journal of Physics and Chemistry of Solids, Vol. 23, pp. 1177-1190, 1962.

7. P. Coleman and S. Green, "Millimeter and Submillimeter Wavelength Receiver Techniques," Electronics System Division (RADC), Final Report, September 1968.